Extracting of Shoreline in Baltim Beach Using Remote Sensing and Global Positioning System (Gps) Techniques

تغير خط الشاطئ لمصيف بلطيم باستخدام الصور الفضائية للقمر الصناعى الجديد ونظام الرصد العالمى الدقيق

Bahaa A. El-Sharnouby[1], Kassem S. El-Alfy[2], Osami S. Rageh[3],
Mohammed M. El-Sharabasy[4]

1. Prof., of Harbor Engineering, Faculty of Engineering, Alexandria University, Egypt.
2. Prof., of Hydraulics, Irrigation & Hydraulics Dept., Faculty of Engineering, Mansoura University, Egypt.
3. Prof., of Harbor Engineering, Faculty of Engineering, Mansoura University, Egypt.
4. Ph.D. Student, Irrigation & Hydraulics Dept., Faculty of Engineering, Mansoura University, Egypt.

خلاصة

مصيف بلطيم من اهم المصايف المشهورة فى منطقة دلتا نهر النيل-مصر. الكثير من هذه المواقع تحتاج الى فترات طويلة ومجهود كبير للحصول على بيانات وتحليلها لحساب التغير فى خط الشاطئ. لذلك يقدم البحث طريقة تمتاز بالتكلفة والمجهود الاقل عن طريق الصور الفضائية للقمر الصناعى الجديد (2013) . تم عمل معالجة للصور وتجميع للطبقات لتحسين الرؤية باستخدام (layer stack function) ورسم خط الشاطئ عن طريق نظام المعلومات الجيوغرافية والاستشعار عن بعد. تم استخدام نظام الرصد العالمى الدقيق لقياس التغير فى خط الشاطئ لمصيف بلطيم باستخدام جهازين. الجهاز الاول ثابت فى مكان معلوم الاحداثيات والجهاز الثانى متحرك على خط الشاطئ ومتصل باثنى عشر قمر صناعى على الاقل . تم تجيع البيانات من المرصد الثابت وجهاز الاستقبال المتحرك وعمل معالجة للاخطاء للحصول على دقة عالية فى القياس باستخدام برنامج (Lecia Office Software) . أيضا تم عمل مقارنة بين الصور الفضائية للقمر الصناعى ونظام الرصد العالمى الدقيق لنفس الفترة الزمنية (2014-3-24) لقياس التغير فى خط الشاطئ.وقد أوضحت الدارسة ان هناك ارتباط قوى بين الطريقتين لتمثيل خط الشاطئ.

ABSTRACT

Baltim beach is one of the most important public beaches fronting the central sector of the Nile Delta, Egypt. Many site and region specific shoreline change monitoring programs use labor and time intensity methodologies for data collection. The collection, compilation, and analysis of this data can take years. This study presents a low cost methodology for quantifying regional shoreline change using Landsat-8 **Operational Land Imager (OLI)** data. This paper compares multi-spectral imagery from landsat-8 with that of the **Global Positioning System (GPS)** surveying techniques when used to extract shoreline for Baltim beach. The latest in the Landsat series of satellites was launched February 11, 2013. Image processing techniques have been carried out to enhance the image resolution by the layer stack function using **ERDAS** Imagine, 2013. The best results from multispectral data were obtained using remote sensing and **Geographic Information System (GIS)** based on a combination of histogram thresholding and band ratio techniques. Kinematic **GPS** measurements are made with two GPS receivers, one of which is fixed (base station) located over a known fixed point and the other is moving on shoreline (rover). The data collected by the rover are processed and corrected after taking measurements then post-processed to achieve very high accuracy (sub meters) using **Lecia Office Software**. Using Landsat-8 OLI's imagery data analysis showed a good agreement with the global position system (GPS) surveying techniques for extraction of Baltim shoreline.

Keywords: Baltim, Landsat 8, GPS, ERDAS Imagine, GIS, Shoreline.

1. INTRODUCTION

A shoreline is defined as the line of contact between land and water. It is one of the rapidly changing linear features of the coastal zone which is dynamic in nature. The methods of shoreline extraction divided into four categories; (i) conventional ground surveying; (ii) modern numerical technology; (iii) airborne imagery; and (iv) satellite imagery. All of these methods have both advantages and disadvantages. Although ground survey is the most conventional and accurate method, it is time-consuming and is cost-effective (needs intensive labor, and restricted by the difficulty of access). Recently, remote sensing and GIS have been widely used as another option than conventional methods for monitoring shoreline position. Further, the satellite imagery has many advantages over aerial photography. For example, the satellite is operational all the time of the year and captures the image of the same area with certain frequency. Satellite image also captures larger areas with relatively high resolutions.

Many researchers use the remote sensing techniques to study the coastal changes along the Nile Delta Coast especially around Rosetta and Damietta promontory. **Alesheikh et al.,(2007)** evaluated the accuracy of remote sensing techniques and a ground truth map for extracted the coastline of Urmia lake and Hyersaline lake using three Landsat 7 ETM+ images; three Landsat 5 TM images;three Landsat 4 TM images**. EL-Banna and E. Hereher (2009)** detected temporal shoreline changes and erosion-accretion rates, using remote sensing, and their associated sediment characteristics along the coast of North Sinai, Egypt. **Frihy and Dewidar (2010)** used the Landsat Multi-spectral Scanner (MSS) and (ETM+) digital data to monitor coastal changes along the North-eastern Nile Delta. **EL-Asmar and El-Hereher (2010)** investigated the change detection of the coastal zone east of the Nile Delta using a set of four satellite images from the multi-spectral scanner (MSS), thematic mapper (TM) and systems Pour Observation de la Terre (SPOT). **CHUANMIN el al.,(2011)** presents shoreline changes in west-central Florida between 1987 and 2008 using nine Landsat Thematic (TM) images. **Dewidar (2011)** presented shoreline maps illustrating the shoreline erosion accretion pattern in the coastal area between Marsa-Alam and Hamata of Red Sea coastline by using different sources of remote sensing data, Landsat MSS (1972), Landsat TM (1990), Landsat ETM+ (1998, 2000) and Terra Aster (2007) satellite images were used. **Tawfik (2012)** used the different characteristics of the Landsat missions by USGS to detect shoreline changes around Rosetta promontory. **EL-Asmar et al (2012)** used images from different satellites sensors MSS, TM, SRTM from 1973 to 2003. . **Mahapatra et al., (2013)** investigated the shoreline changes along the South Gujarat coast using multi temporal satellite images of Landsat MSS (1972), Landsat TM (1990), Landsat ETM (2001) and IRS P6, LISS-IV (2011). **Ali Niya et al.,(2013)** investigated shoreline detection for Persian Gulf in Bushehr provinvce,Iran using remote sensing and Gis, The digital images used two Landsat 7 ETM+ images and one Landsat 5 TM images.
and presented the major environment hazards facing the coastal wetlands (Manzala and Burullus) of the Nile Delta.

According to Landsat website, Landsat-8 is the latest NASA satellite in a series that has produced an uninterrupted multispectral record of the Earth's land surface since 1972. Along with data acquisition and the USGS archival and distribution systems, the program includes the data processing techniques required to render the Landsat 8 data into a scientifically useful form. ERDAS Imagine software was used to perform image processing of satellite image. In addition image digitizing was applied for delineating the shoreline trend at the study

area using the ArcGIS V. 10.1 Software Package.

GPS had become a standard surveying technique in most surveying practices due to its ease and precision. The techniques that are commonly used now (field data methods) are Static positioning, Fast Static positions, Post-Processed Kinematic (PPK) positioning and Real-Time Kinematic (RTK) positioning. Post-processed kinematic (PPK) surveys are generally used for mapping or for surveying points where only several cm of precision are needed, such as mapping out a feature such as a flat scarp or a shoreline. Occupation times for survey points are on the order of seconds. Data must be post-processed to achieve high-precision results; this requires a processing program **using Lecia Office Software.**

2. STUDY AREA

The study area shoreline lies between 31°30′00″N to 31°40′00″N latitudes (3492000 to 3600000) and 31°00′00″E to 31°15′00″E longitudes (318000 to 328000). **Baltim** beach is one of the most important public beaches fronting the central sector of the Nile Delta and is located about 11.5km east of the Burullus lagoon inlet as shown in Figure (1). **Baltim** resort is located on a very active convex shoreline. According to accepted coastal sediment transport principles, concave shorelines areas of transport convergence and accrete, whereas convex shoreline segments (promontories) erode. **Baltim** beach remained unprotected until 1992, at which time construction of protective breakwaters commenced. Off this coastline, a total of 14 shore-parallel detached breakwaters have been constructed in four phases between 1993 and 2007. Nine breakwaters (4-7 ton dolos, 250-350m length, 220m far from the coast, 300-400m gap between each other, 3-4m water depth, and 2.5m crest level) were constructed between the years 1993-2002. Additional five breakwaters were constructed after 2003 with the same characteristics. Moreover short nine groins (75-100m length, and 250-300m apart) were constructed on the eastward up to Kitchener drain between the years 2008-2013. Landsat image is presented in Figure (2), showing the fourteen detached breakwaters and the nine short groins. Also, the dimension of detached breakwaters and groins are presented in Figure (3). **Kitchener Drain** excavated between 1930 and 1940, lies in the eastern limit of the study area and flows south to north. This drain 70km long and 60m width, discharges an amount of about $2 \times 10^5 m^3$/year drainage water into the sea.
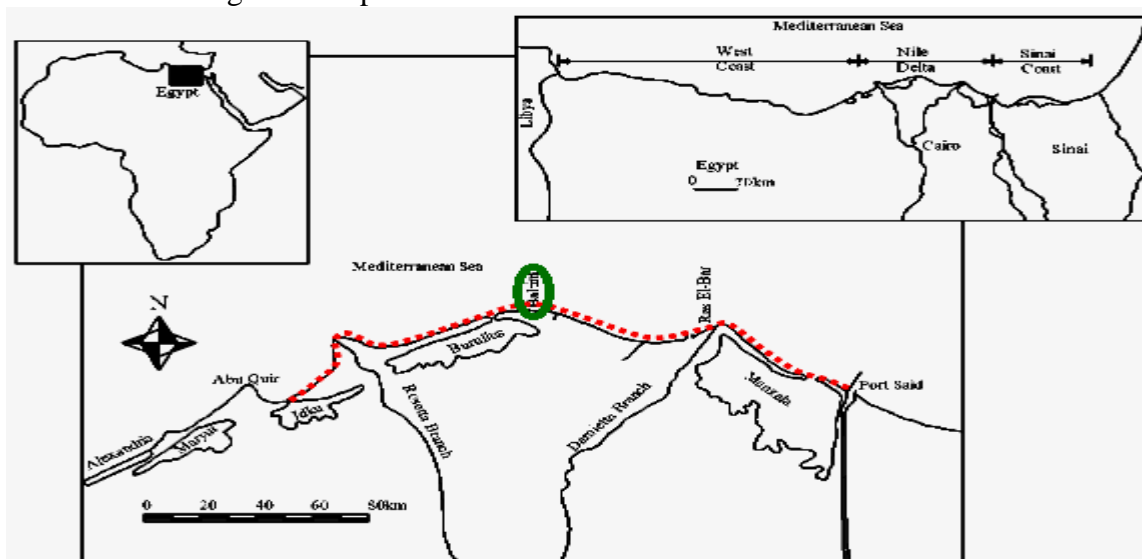

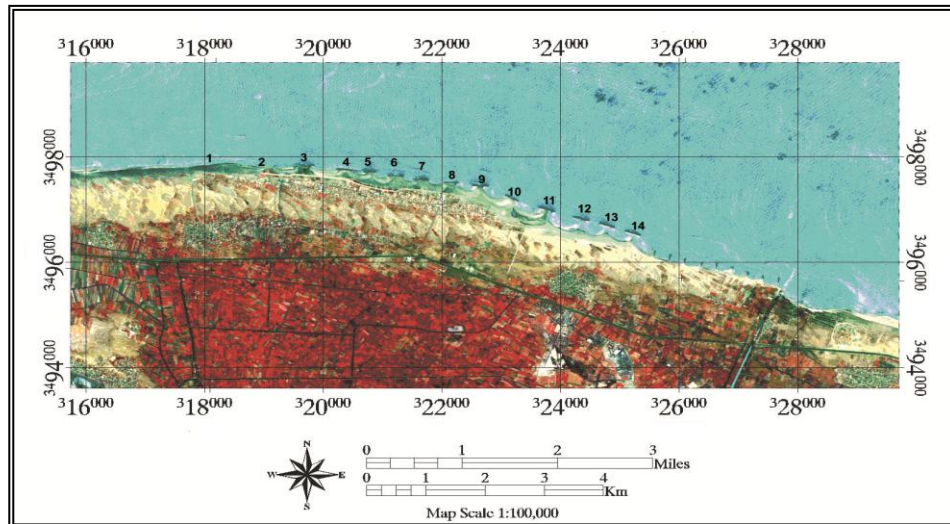**Fig.1:** Location of Baltim Beach along the Nile Delta Coast

Fig. 2: Map of the study area.

3. MATERIAL AND METHODS

3.1. Tidal Data and Their Influence on Determination of Coastline

Among the cyclical variations, tides cause rapid sea level variations; therefore, it is fundamental to evaluate such effects during the image acquisitions to locate the free-surface level. Tides are due to astronomic and meteorological phenomena. In particular, the astronomic tide is due to the gravitational attraction of sun and moon (30% and 70% respectively). It is evaluated by applying the so called harmonic method, that considers the sum of tidal components represented by sinusoidal waves seven components (four semi-diurnal and three diurnal) are enough to have an approximation of one centimeter (**NATIONAL OCEANIC AND ATMOSPHERIC ADMINISTRATION, 1982).** Since the selected images were acquired in good weather conditions (calm sea), we neglected the influence of meteorological tide. Tide conditions for our dataset were evaluated using the freeware wxtide32 program (http://www.wxtide32.com/). For the study area, the oscillations of water level (only due to astronomic tide) range between 19 and 46cm in a semi-diurnal behavior (oscillation time of about 12 h and 25 min) characterized by two maxima and two minima that are not coincident as shown in Figure (4) and Table (1).

3.2. Dataset for Landsat Image

In order to extract shoreline along Baltim area, 11-band landsat-8, OLI imagery used in this study were downloaded from the U.S. Geological Survey (USGS). Satellite data were acquired at no cost from the USGS on-line open resources (http://usgs.gov/EarthExplorer).

3.3. Landsat Spectral Band Information

Landsat images are composed of 11 different bands, each representing a different portion of the electromagnetic spectrum. Landsat-8 OLI sensor includes a new coastal-aerosol band (band1), which can be used with two other bands for closer investigations of coastal waters and estimating the concentration of aerosols in the atmosphere. In order to work with Landsat bands, we discuss the specifications of each band, figure (5).
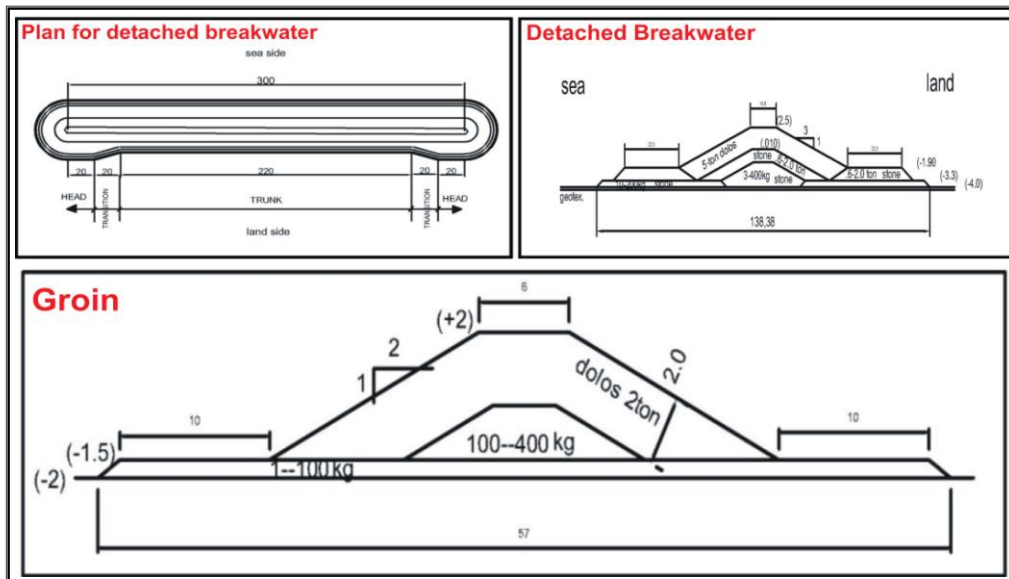
Fig. 3: Dimensions and cross section of detached breakwaters and groins.

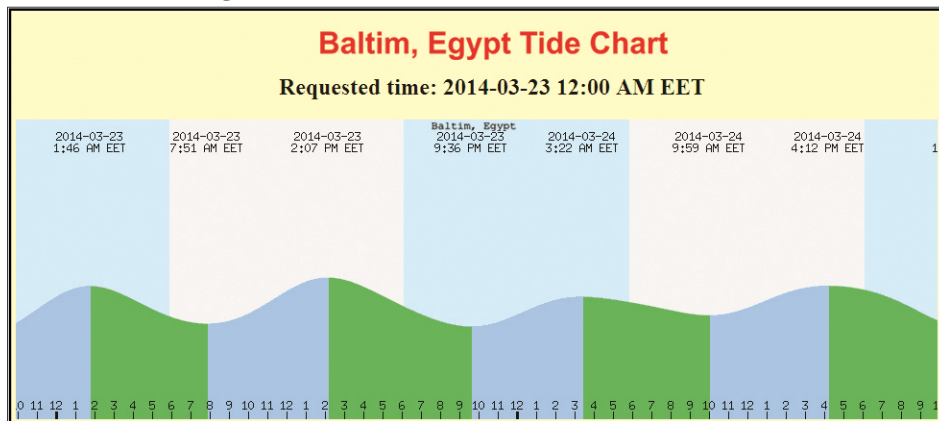**Fig. 4:** The values of tide in Baltim area in 23-3-2014.

Table 1: Minimum and maximum values of tide for Baltim area.

Date	Time	Height	State
2014-03-23	1:46 AM	0.40 meters	High tide
2014-03-23	7:51 AM	0.28 meters	Low tide
2014-03-23	2:07 PM	0.42 meters	High Tide
2014-03-23	9:36 PM	0.27meters	Low tide
2014-03-24	3:22 AM	0.36meters	High tide
2014-03-24	9:59 AM	0.30meters	Low tide
2014-03-24	4:12 PM	0.40meters	High tide
2014-03-24	11:43 PM	0.26meters	Low tide
2014-03-25	6:51 AM	0.38meters	High tide
2014-03-25	12:10 PM	0.29meters	Low tide
2014-03-25	6:47 PM	0.42meters	High tide
2014-03-26	1:07 AM	0.23meters	Low tide
2014-03-26	7:47 AM	0.43meters	High tide
2014-03-26	1:25 PM	0.25meters	Low tide
2014-03-26	7:47 PM	0.46meters	High tide
2014-03-27	2:00 AM	0.19meters	Low tide

3.4. Common Landsat Band Combinations

Individual bands can be composited in a Red, Green, and Blue (RGB) combination in order to visualize the data in color. The registered imageries were opened in ARC GIS 10.1 environment with a band combination of 3:2:1 (RGB) for displaying best contrast between land-water boundary in the satellite image and thus shoreline was identified and demarcated. Displayed below are some common band combinations in RGB Landsat 8,as shown in figure(6).

3.5. Geometric Corrections

The image data were geometrically corrected according to the Universal Transverse Mercator (UTM) map projection system; zone 36 north, using 25 ground control points (GCPs) that were selected at well-known features using a Geographic Information System (GIS).

3.6. Image Processing and shoreline extraction

Image processing was performed using **ERDAS** Imagine, 2013. The layer stack function is useful for placing layers one on top of the other. It is especially useful now that Landsat satellite data are being released in full-scene, one-layer-per-image files. Also, Landsat 8 files often come in one-band-per-image files, and this procedure will work as well, but Landsat 8 band 6 (thermal) typically has 60-meter resolution, and the panchromatic band typically has 15-meter resolution, while the other bands have 30-meter resolution. If the panchromatic band is stacked into the output file, bands 1 through 7 will be resampled to 15-meter pixel size, and some spectral definition will be lost. The file size more than quadrupled is shown in figure (7). For Landsat 8 data, layer stack bands 1through 5 and band 7. The panchromatic band and band 6 are kept as separate files. The defined shoreline perimeter of the coast was digitized on screen from the satellite images in geographic information system using ARCGIS software version 10.1. Figure (8) illustrates the work flow of the entire system of shoreline analysis based on satellite images

4. SURVEYING WITH GPS

Advantages of GPS surveys are Three Dimensional, Site Indivisibility Not Needed, Weather Independent, Day or Night Operation, Common Reference System, Rapid Data Processing with Quality Control High Precision, and Very Few Skilled Personnel Needed. The techniques that are commonly used now (field data methods):

Static Positioning: Static positioning typically uses a network or multiple baseline approach for positioning. It may consist of multiple receivers, multiple baselines, multiple observational redundancies and multiple sessions. A least squares adjustment of the observations is required. This method provides the highest accuracy achievable and requires the longest observation times.

Fast-Static Positioning: This method requires shorter occupation times (i.e. 5 to 20+ minutes) than static positioning and may use a radial baseline technique, network technique, or a combination of the two. Fast static requires a least squares adjustment or use of processing software capable of producing a weighted mean average of the observations.

Post-Processed Kinematic (PPK) Positioning: Post processed kinematic survey methods provide the surveyor with a technique for high production Cadastral Measurements and can be used in areas with minimal obstructions of the satellites. PPK uses significantly reduced observation times compared to static or fast-static observations. This method requires a least squares adjustment or other multiple baseline statistical analysis capable of producing a weighted mean average of the observations.

Real-time Kinematic (RTK) Positioning: Real-time kinematic positioning is similar to a PPK or a total station radial survey. RTK does not require post-processing of

the data to obtain a position solution. This allows for real-time surveying in the field. This method allows the surveyor to make corner moves (stake out) similar to total station data collector methods.

Table 2: Acquired data, sensor type and spatial resolution of Landsat sensors data used in this study.
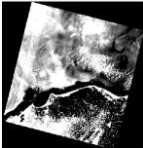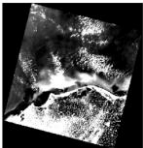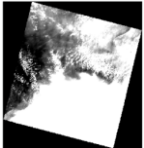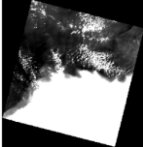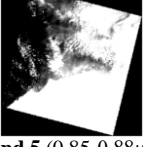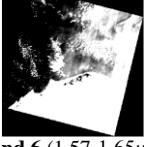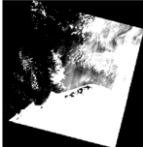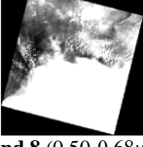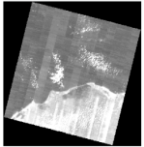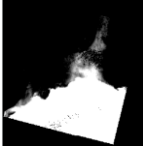
Satellite	Sensor	Scene Path/row	Date	Spatial resolution (meters)
Landsat 8	Oli/TiRs	177/38	23-3-2014	30m

Band 1 (0.43-0.45μm) Bathymetric mapping; distinguishes soil from vegetation, deciduous from coniferous vegetation.

Band 2 (0.45-0.51μm) Emphasizes peak vegetation, which is useful for assessing plant vigor.

Band 3 (0.53-0.59μm) Emphasizes biomass content and shorelines.

Band 4 (0.64-0.67μm) Emphasizes vegetation types.

Band 5 (0.85-0.88μm) Discriminates moisture content of soil and vegetation; penetrates thin clouds.

Band 6 (1.57-1.65μm) Useful for thermal mapping and estimated soil moisture.

Band 7 (2.11-2.29μm) Useful for mapping hydrothermally altered rocks associated with mineral deposits.

Band 8 (0.50-0.68μm) A panchromatic band (visible through near infrared) with 15-meter resolution for "sharpening" of multispectral images.

Band 9 (1.36-1.38μm) it's designed especially for cirrus clouds

Band 10 (10.6-11.19 μm) Is in the thermal infrared, or TIR – they see heat. Instead of measuring the temperature of the air

Band 11 (11.5-12.51μm) Is in the thermal infrared, or TIR – they see heat. Instead of measuring the temperature of the air

Fig. 5: Landsat Spectral Band for Landsat 8.
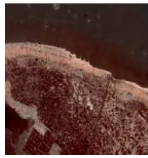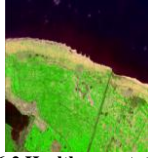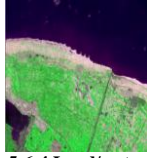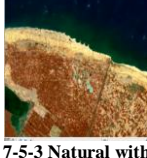
4-3-2 (Natural Color)　　7-6-4 False color (urban)　　5-4-3 Color infrared (vegetation)　　6-5-2 Agriculture　　7-6-5 Atmospheric penetration

5-6-2 Healthy vegetation　　5-6-4 Land/water　　7-5-3 Natural with atmospheric removal　　7-5-4 Shortwave infrared　　6-5-4 Vegetation analysis

Fig. 6: Band combination for Landsat 8.
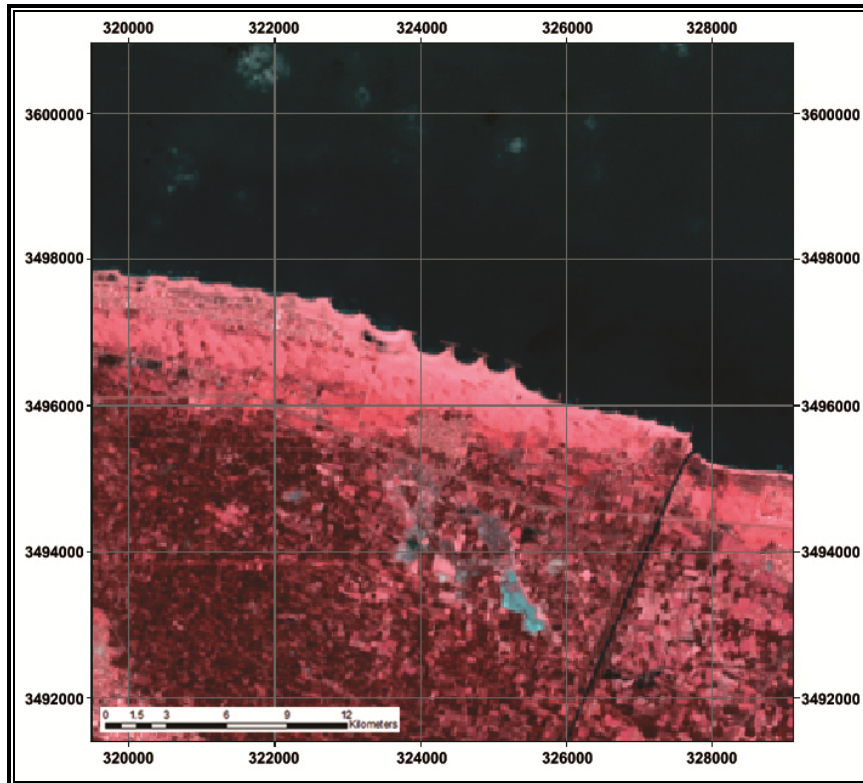
Fig. 7: Landsat image for Baltim beach after Layer stack.
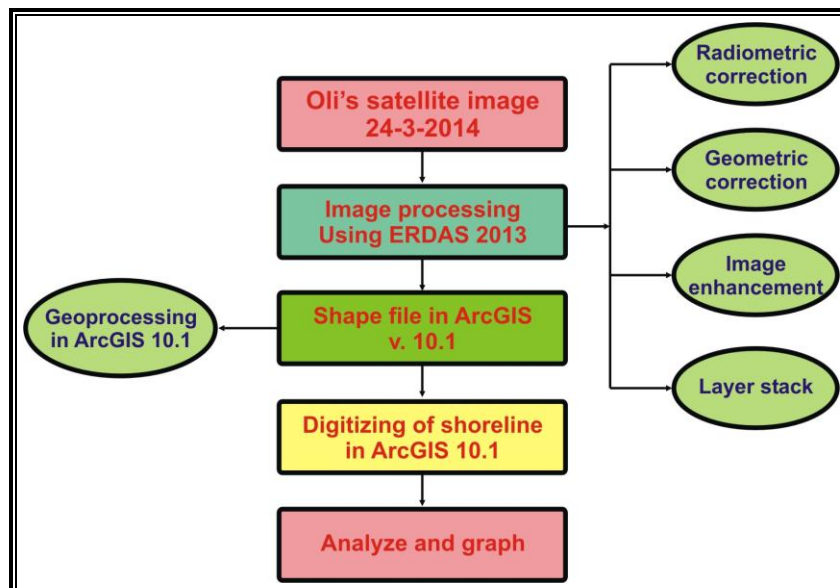
Fig. 8: Diagram of the present study workflow.

Today, Real Time Kinematic (RTK) and Post-Processed Kinematic (PPK) techniques are widely used for the measurement of details on the shore line. So, the measurements in this study obtained by post-processed Kinematic. (PPK). PPK surveys require data from at least two receivers: a 'base' (reference) receiver and a 'rover' (moving) receiver. **Reference**, the base GPS antenna can be set up over an existing mark or a newly establis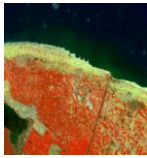hed mark, or, if no repeat surveying will be needed, placed directly on the ground. Correspondingly, the antenna mount used (if any) will depend on project needs. For a repeatable survey, you will

need a way to center and level the antenna over your mark. If you are establishing a base marker for the first time, plan to collect at least an hour's worth of data. While other (rover) GPS units are moved from station to station according to a

sketch for Baltim beach to determine the occupied points as shown in Figure (9). All baselines are produced from the GPS unit occupying a reference station to the rover units as shown in Figure (10).
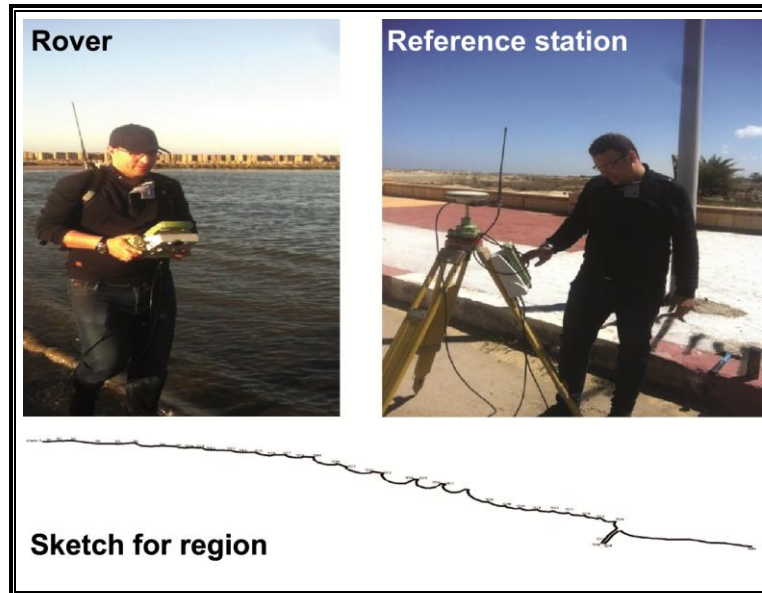
Fig. 9: A reference station, rover (moving point) and sketch for occupied points.
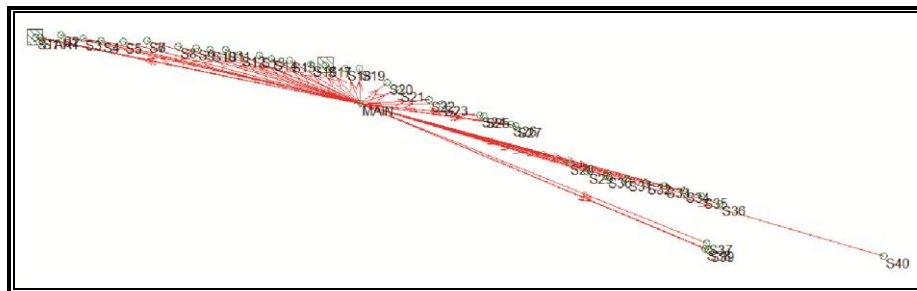
Fig. 10: Baseline between reference point and rover points.

5. RESULTS AND DISCUSSIONS

Shoreline is one of the important dynamic coastal features where the land, air and sea meet. In any open coast, when manmade structures such as breakwaters interfere with the littoral currents, shoreline changes drastically. Using ArcGis v 10.1, a shape file constructed to obtain the coordinates and represent the shape of erosion and acceleration for baltim beach is shown in figure (11). This Figure shows that after the following construction of fourteen detached breakwaters, accretion has become the dominat process with the formation of

rapid tombolos on the leeward side of theses structures. This accretion has filled the down area between the shoreline and the breakwaters. The plan form of the formed tombolo indicates that these accretionary features have been developed from the prevailing longshore current to the east. Also, the construction of these detached breakwaters with the different characteristics of length, width, spacing between them, angle of detached breakwaters and spacing between the coastline lead to stable pocket beaches, good protection, poor water quality, poor aesthetic appearance, unsafe for swimmers and lee side erosion. In other words, the

bulge formation of the tombolo has eventually transformed the breakwater system to act as a shore-parallel seawall. For the lee side erosion in this region, the nine short groins built downcoast of the fourteen detached breakwaters system particularly east of the kitchener drain stabilize the 5km shoreline sector. But, Landsat images shows the local erosion behind the kitchener drain. The downcoast erosion east of the kitchener drain was resulted from the interruption of the unidirectional easterly sediment transport by the breakwater system and their associated tombolo formations, thus increasing sand starvation of downcoast beaches of this region.

Correction of collected data using Lecia Geo Office 5.0 let us achieve high precision of 1cm±1ppm. This correction is possible because the base station is located over a stationary point with known coordinates and any deviations from this position can be considered noise and can be removed. The difference in coordinates between the base station may then be analyzed together with data from the rover to obtain an accurate positioning of the rover relative to the base station. Figures (12 a,b) show the time of measurement for reference and rover points for each occupied points which all manually occupied points are 40 and the quality of points for height and position reaches about ±0.01m.
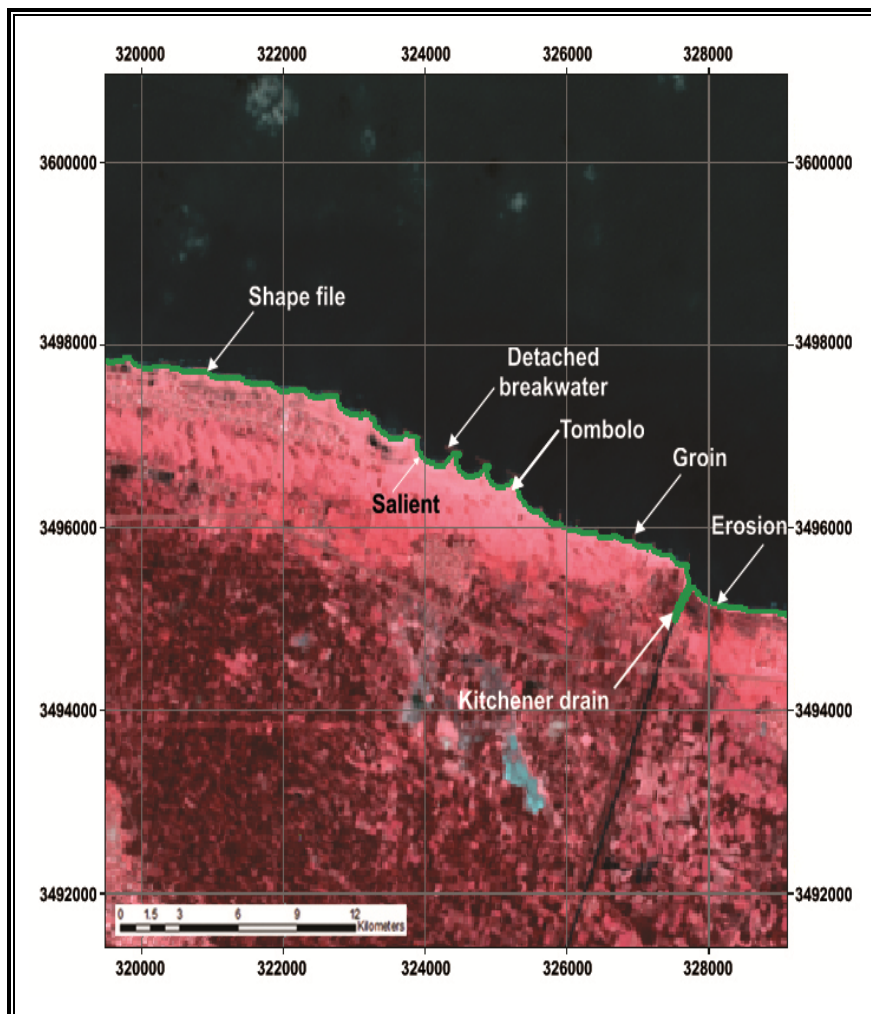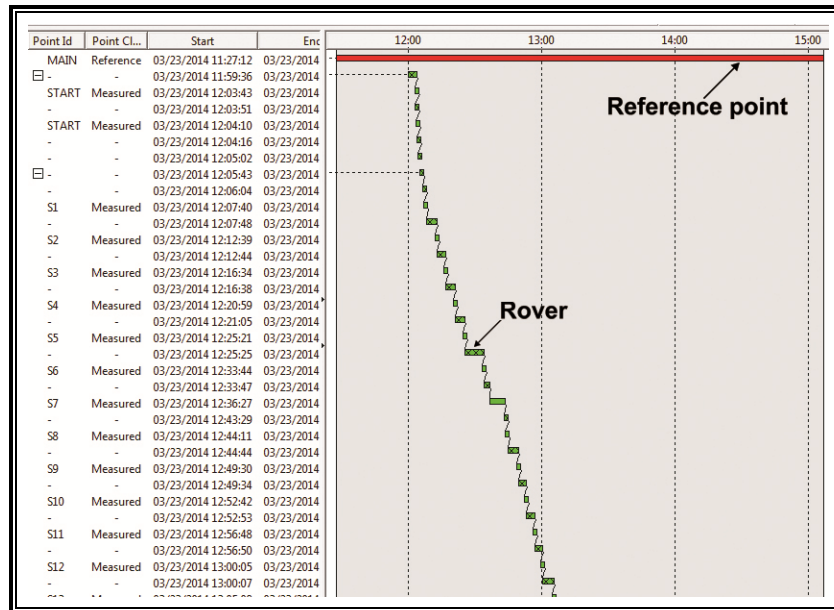

Fig. 11: Shape file of Baltim beach.

Point Id	Point Cl...	Start	End
MAIN	Reference	03/23/2014 11:27:12	03/23/2014
-	-	03/23/2014 11:59:36	03/23/2014
START	Measured	03/23/2014 12:03:43	03/23/2014
-	-	03/23/2014 12:03:51	03/23/2014
START	Measured	03/23/2014 12:04:10	03/23/2014
-	-	03/23/2014 12:04:16	03/23/2014
-	-	03/23/2014 12:05:02	03/23/2014
-	-	03/23/2014 12:05:43	03/23/2014
-	-	03/23/2014 12:06:04	03/23/2014
S1	Measured	03/23/2014 12:07:40	03/23/2014
-	-	03/23/2014 12:07:48	03/23/2014
S2	Measured	03/23/2014 12:12:39	03/23/2014
-	-	03/23/2014 12:12:44	03/23/2014
S3	Measured	03/23/2014 12:16:34	03/23/2014
-	-	03/23/2014 12:16:38	03/23/2014
S4	Measured	03/23/2014 12:20:59	03/23/2014
-	-	03/23/2014 12:21:05	03/23/2014
S5	Measured	03/23/2014 12:25:21	03/23/2014
-	-	03/23/2014 12:25:25	03/23/2014
S6	Measured	03/23/2014 12:33:44	03/23/2014
-	-	03/23/2014 12:33:47	03/23/2014
S7	Measured	03/23/2014 12:36:27	03/23/2014
-	-	03/23/2014 12:43:29	03/23/2014
S8	Measured	03/23/2014 12:44:11	03/23/2014
-	-	03/23/2014 12:44:44	03/23/2014
S9	Measured	03/23/2014 12:49:30	03/23/2014
-	-	03/23/2014 12:49:34	03/23/2014
S10	Measured	03/23/2014 12:52:42	03/23/2014
-	-	03/23/2014 12:52:53	03/23/2014
S11	Measured	03/23/2014 12:56:48	03/23/2014
-	-	03/23/2014 12:56:50	03/23/2014
S12	Measured	03/23/2014 13:00:05	03/23/2014
-	-	03/23/2014 13:00:07	03/23/2014

Reference point

Rover

Fig. 12(a): The time of measurement for reference, rover.

Point Id	Point Class	Date/Time	Easting	Northing	Ellip. Hgt.	Ortho. Hgt.	Geoid Sep.	Posn. Qlty	Hgt. Qlty	Posn. + Hgt. Qlty
START	Measured	03/23/2014 12:04:10	318352.8174	3497879.0209	21.9895	-	-	0.0039	0.0073	0.0083
S1	Measured	03/23/2014 12:07:40	318420.4825	3497876.7081	21.7738	-	-	0.0052	0.0094	0.0107
S2	Measured	03/23/2014 12:12:39	318693.6331	3497910.6977	21.8597	-	-	0.0086	0.0146	0.0169
S3	Measured	03/23/2014 12:16:34	319001.7764	3497873.7188	21.8238	-	-	0.0046	0.0074	0.0087
S4	Measured	03/23/2014 12:20:59	319251.9254	3497834.4791	21.8727	-	-	0.0073	0.0111	0.0133
S5	Measured	03/23/2014 12:25:21	319551.5971	3497825.5510	22.1469	-	-	0.0078	0.0113	0.0137
S7	Measured	03/23/2014 12:36:27	319876.9708	3497837.0364	21.8015	-	-	0.0252	0.0292	0.0386
S6	Measured	03/23/2014 12:33:44	319877.9391	3497838.6688	21.8102	-	-	0.0152	0.0174	0.0231
S8	Measured	03/23/2014 12:44:11	320305.0562	3497759.5428	21.7683	-	-	0.0037	0.0045	0.0058
S9	Measured	03/23/2014 12:49:30	320543.2952	3497736.4907	21.7690	-	-	0.0127	0.0157	0.0202
S10	Measured	03/23/2014 12:52:42	320741.6706	3497715.1101	21.8348	-	-	0.0076	0.0096	0.0122
S11	Measured	03/23/2014 12:56:48	320948.5397	3497710.0762	21.8701	-	-	0.0071	0.0092	0.0116
S12	Measured	03/23/2014 13:00:05	321143.6657	3497644.6396	21.7577	-	-	0.0042	0.0055	0.0069
S13	Measured	03/23/2014 13:05:08	321412.9745	3497632.6467	21.7193	-	-	0.0125	0.0176	0.0216
S14	Measured	03/23/2014 13:07:40	321573.2027	3497585.3034	21.7288	-	-	0.0103	0.0138	0.0172
S15	Measured	03/23/2014 13:12:45	321828.2461	3497567.3936	21.5505	-	-	0.0054	0.0082	0.0098
S16	Measured	03/23/2014 13:17:37	322117.2581	3497507.5220	21.4737	-	-	0.0044	0.0075	0.0087
S17	Measured	03/23/2014 13:24:15	322319.3343	3497504.1334	21.9384	-	-	0.0039	0.0069	0.0079
S18	Measured	03/23/2014 13:34:59	322590.9898	3497450.9482	21.6754	-	-	0.0042	0.0081	0.0091
S19	Measured	03/23/2014 13:37:44	322772.6024	3497451.3335	21.7465	-	-	0.0049	0.0097	0.0109
MAIN	Reference	03/23/2014 11:27:12	322784.3370	3496972.6529	23.2395	-	-	0.9020	1.3875	1.6549
S20	Measured	03/23/2014 13:44:45	323161.1853	3497259.6008	21.7103	-	-	0.0038	0.0086	0.0094
S21	Measured	03/23/2014 13:48:05	323311.9641	3497166.9547	21.7341	-	-	0.0042	0.0098	0.0107
S22	Measured	03/23/2014 15:26:54	323725.2206	3497029.2136	21.7803	-	-	0.0104	0.0198	0.0224
S23	Measured	03/23/2014 15:29:52	323907.0191	3496974.2490	21.8699	-	-	0.0055	0.0091	0.0106
S24	Measured	03/23/2014 15:39:18	324426.0014	3496815.9456	21.5566	-	-	0.0037	0.0063	0.0073
S25	Measured	03/23/2014 15:40:53	324477.2685	3496802.1643	21.5617	-	-	0.0031	0.0054	0.0062
S26	Measured	03/23/2014 15:48:40	324855.3803	3496689.3605	21.6345	-	-	0.0025	0.0045	0.0052
S27	Measured	03/23/2014 15:50:05	324920.9779	3496666.9496	21.6676	-	-	0.0099	0.0175	0.0201
S28	Measured	03/23/2014 16:04:06	325636.4905	3496166.4736	21.7722	-	-	0.0046	0.0088	0.0099
S29	Measured	03/23/2014 16:10:45	325890.0128	3496044.0440	21.7607	-	-	0.0056	0.0110	0.0124
S30	Measured	03/23/2014 16:16:03	326152.4545	3495987.2568	21.7743	-	-	0.0059	0.0122	0.0135
S31	Measured	03/23/2014 16:20:32	326427.9466	3495938.3075	21.8132	-	-	0.0058	0.0162	0.0181
S32	Measured	03/23/2014 16:24:41	326686.7020	3495899.5047	21.7185	-	-	0.0064	0.0128	0.0143

Fig. 12(b): The quality of points.

Figure (13) shows the sample of resulted geographic coordinates after processing for moving points. The total moving points are 13722. After data processing, data is transferred to global mapper to reshape the shoreline and convert to ArcGIS in order to apply this line in Landsat image. The accuracy of the two methods is then tested (presented shape file resulted from Landsat 8 techniques with the lines resulted from GPS surveying). It is found that an apparent decrease in the difference of the polylines with error 8% between two method as shown in figure (14). Also,

figure (15) display Landsat image technique and Global position system (GPS) surveying on layer stacking image.

6. CONCLUSIONS

This paper compares between two methods of shoreline extraction for baltim beach. The first method is Landsat-8 imagary. The second method is conventional ground surveying using Global Position System (GPS) surveying. For Landsat image obtained by the U.S. Geological Survey (USGS) in 23-3-2014. Also, This Landsat image has been

processed using ERDAS Imagine software, 2013 by using a Layer Stack Function which is useful for placing layers one on top of the other to get a best resolution. In addition image digitizing was applied for the shoreline trend at the baltim beach using ArcGIS V. 10.1 Software Package. The Results show the formation of tombolos and salient in the leeward side of these structures. This accretion has filled the down area between the shoreline and some breakwaters which transformed the breakwater system to act as a shore-parallel seawall and make this region unsafe for swimmers. For Global Position System (GPS) surveying, GPS has become a standard surveying technique in most surveying practices has Advantages are Three Dimensional, Day or Night Operation, Common Reference System, Rapid Data Processing with Quality Control High Precision. The most commonly used GPS data collection technique is used here ,Post-Processed Kinematic (PPK) Positioning. PPK surveys require data from at least two receivers (reference – rover). 40 points are manually occupied using GPS with position quality of about sub meters. The data collected by the rover was post processed using a processing program, Leica Geo Office 5.0. After processing the geographic coordinates for moving points were 13722 for Baltim beach. To test the accuracy of two methods, present shape file resulted from landsat 8 techniques with the lines results from Global position system (GPS) surveying. It is found that an apparent decrease in the difference of the polylines between two method about 8m.
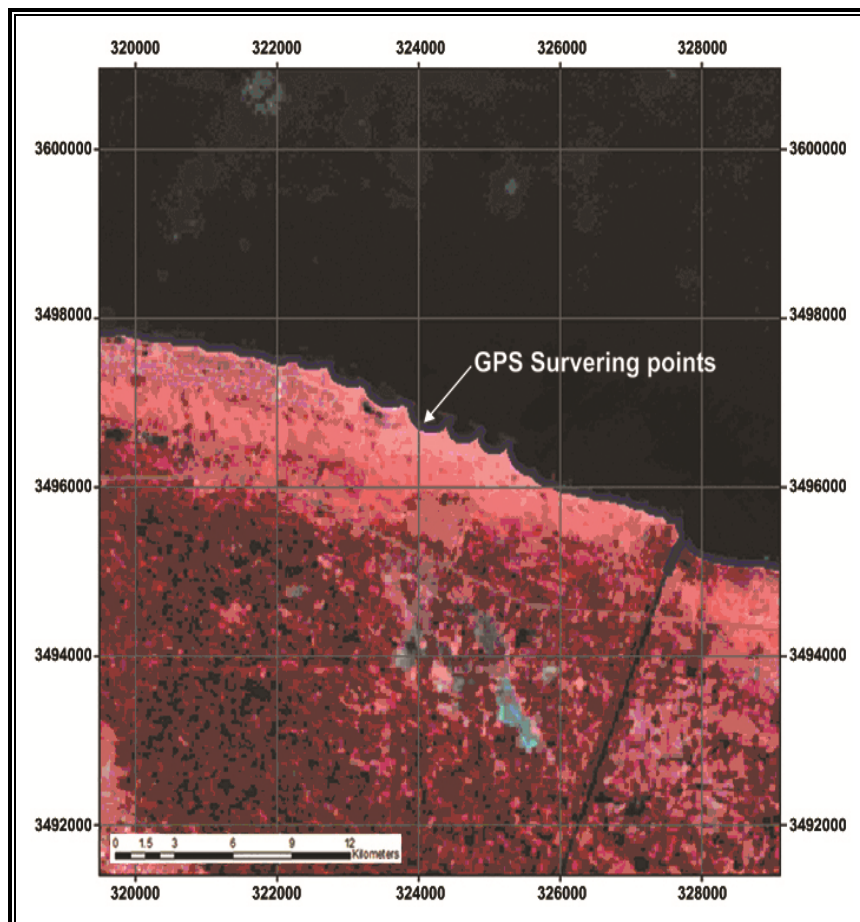

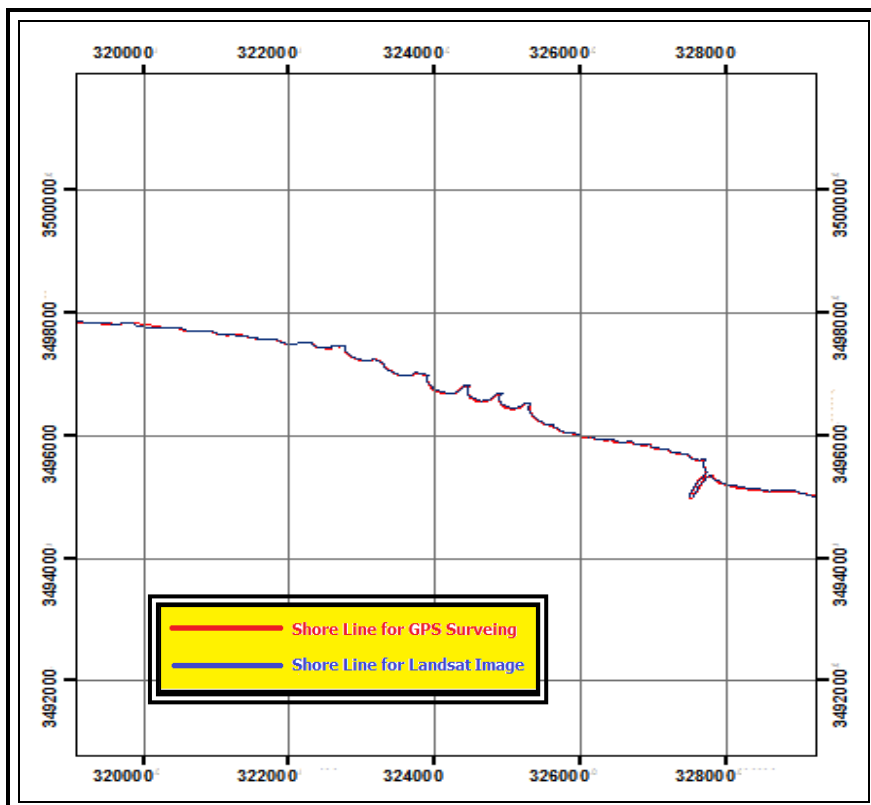**Fig. 13:** Sample of data in Leica Geo Office and ArcGIS.

Fig. 14: Difference between Landsat image technique and Global position system (GPS) surveying.
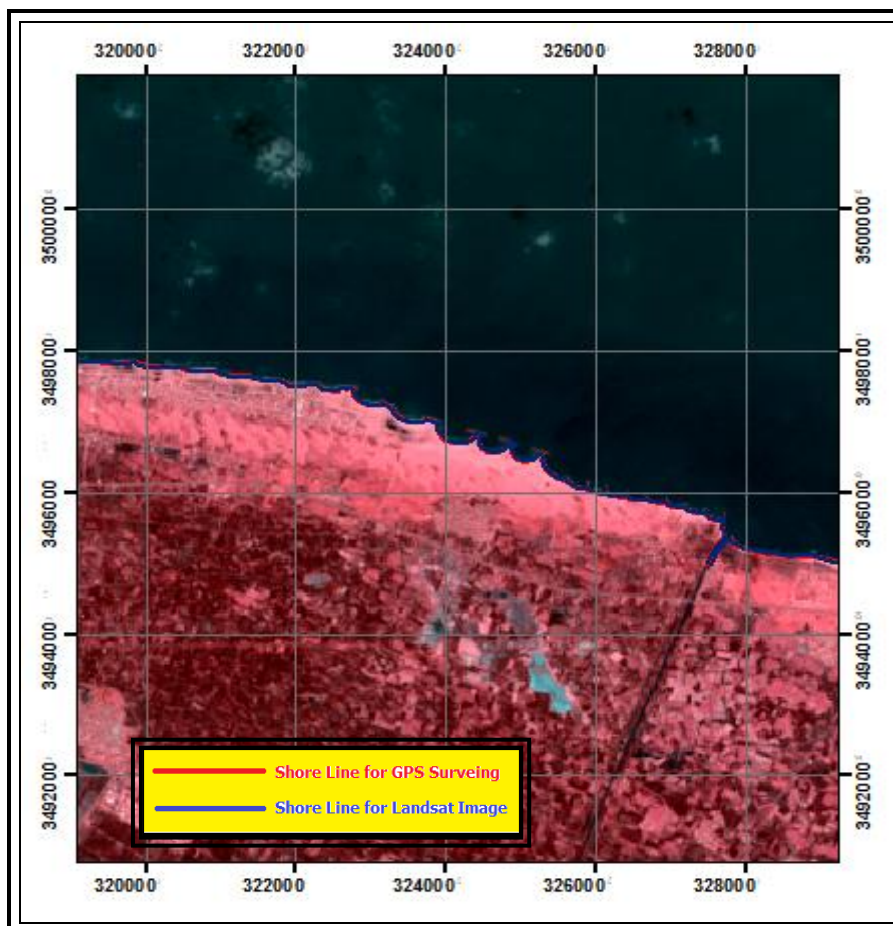

Fig. 15: Landsat image technique and Global position system (GPS) surveying on layer stacking image.

7. REFERENCE

[1] A.A. Alesheikh, A. Ghorbanali and N. Nouri, "Coastline change detection using remote sensing" Int. J. Environ. Sci. Tech., Vol.4, pp. 61-66, 2007.

[2] A.K.Niya et al., "Shoreline Change Mapping Using Remote Sensing and Gis" International Journal of Remote Sensing Applications , Vol. 3, Issue 3, 2013.

[3] H.U. CHUANMIN, E.F. RANK, and I. SOTO, "Shoreline changes in west-central Florida between 1987 and 2008 from Landsat observations" International Journal of Remote Sensing, Vol. 32, pp.8299-8313, 2011.

[4] H.M. EL-Asmar and M.E. Hereher, "Change detection of the coastal zone east of the Nile Delta using remote sensing" Journal of Environmental Earth Science, DOI 10.1007/s12665-010-0564-9, 2010.

[5] H.M. EL-Asmar, M.E. Hereher and S.B. EL-Kafrawy, "Threats Facing Lagoons along the North Coast of the Nile Delta, Egypt" International Journal of Remote Sensing Applications, Vol. 2, pp.24-29, 2012.

[6] Kh.M. Dewidar, and O.E. Frihy, "Automated techniques for quantification of beach change rates using Landsat series along the North-eastern Nile Delta, Egypt" Journal of Oceanography and marina Science,Vol.12,pp.28-39,2010.

[7] Kh.M. Dewidar, "Changes in the Shoreline Position Caused by Natural Processes for Coastline of Marsa Alam and Hamata, Red Sea, Egypt" International Journal of Geosciences, Vol. 2, pp.523-529, 2011.

[8] M.M. ElBanna, "Detecting temporal shoreline changes and erosion/accretion rates, using remote sensing, and their associated sediment characteristics along the coast of North Sinai, Egypt" Journal of Environmental Geology, Vol. 58, pp. 1419-1427, 2009.

[9] M.T. Tawfik, "Analysis and modeling of long-term shoreline changes and alongshore sediment characteristics on the Nile Delta Coast" PhD Thesis, The university of Tokyo, Japan, 169 pp, 2012.

[10] M.Mahapatra el.al, " Shoreline Change Monitoring Along the South Gujarat Coast using Remote Sensing and Gis Techniques" International Journal of Geology,Earth&Environment Sciences,Vol.3,pp115-120,2013.